JOURNAL OF SPACECRAFT AND ROCKETS
Vol. 36, No. 5, September–October 1999

# Flexible Heat Pipes for a Lightweight Spacecraft Radiator

David E. Glass,* Jonathan C. Stevens,† and V. V. Raman‡
*Analytical Services and Materials, Inc., Hampton, Virginia 23666*

**Flexible heat pipes utilizing ultra-high-molecular-weight (UHMW) film wicks and formed UHMW wicks with Kapton® and aluminized Mylar® containers were designed, fabricated, and tested. Wick characterization was performed on both wicks with acetone, methanol, freon, and ethanol. The thin-film UHMW wick had a larger permeability and capillary radius. Burst tests were performed on the Mylar and Kapton heat-pipe containers indicating sufficient strength for the heat-pipe application. The heat pipes were charged with methanol as the working fluid and successfully tested at steady-state conditions. Relatively uniform temperatures were obtained during several days of testing.**

## Nomenclature

| | |
|---|---|
| $Gr$ | = Grashof number |
| $g$ | = acceleration due to gravity |
| $h$ | = heat transfer coefficient, W/m$^2$K |
| $K$ | = permeability, cm$^2$ |
| $k$ | = thermal conductivity, W/mK |
| $L$ | = heat-pipe length, m |
| $P$ | = pressure, dynes/cm$^2$ or kPa |
| $Pr$ | = Prandtl number |
| $q$ | = heat flux, W |
| $r_p$ | = capillary radius, $\mu$m |
| $T$ | = temperature, °C or K |
| $t$ | = time, s |
| $x$ | = wicking height, cm |
| $\beta$ | = orientation relative to the horizontal, deg |
| $\varepsilon$ | = porosity, % |
| $\theta$ | = contact angle, deg |
| $\mu$ | = dynamic viscosity, kg/m-s |
| $\rho$ | = density, g/m$^3$ |
| $\sigma$ | = surface tension, N/m |

*Subscripts*

| | |
|---|---|
| boil | = boiling limit for heat pipe |
| cap | = capillary limit for heat pipe |
| $e$ | = exit |
| ent | = entrainment limit for heat pipe |
| $l$ | = liquid |
| sonic | = sonic limit for heat pipe |

## Introduction

RADIATORS have been used for years in space to dissipate waste heat. To improve the efficiency of the space radiators, heat pipes are used to generate a nearly uniform temperature distribution on the radiator surface. State-of-the-art heat pipes for space radiators are made of a rigid aluminum container with ammonia as the working fluid. The rigid heat pipes are then either bonded to the radiator or embedded in the structure. The coefficient of thermal expansion (CTE) mismatch between the aluminum heat pipe and the lightweight composite radiator panels has been problematic. An alternative heat pipe is studied here that may eliminate the CTE mismatch problems as well as reduce weight and thermal contact resistance problems.

Received 27 January 1998; revision received 4 January 1999; accepted for publication 8 January 1999. 

*Senior Scientist, 107 Research Drive. Senior Member AIAA.

†Research Scientist; currently Research Associate, Department of Applied Science, College of William and Mary, Williamsburg, VA 23187-8795.

‡Research Scientist, 107 Research Drive.

Heat pipes have been used for thermal control in space for many years and the literature has numerous references dealing with the fabrication and testing of heat pipes for space use. A description of several of the space heat pipes is given next.

A self-deploying membrane heat pipe was designed and fabricated using a Mylar® container in the condenser and aluminum in the evaporator, a polyester fabric wick, and R-11 ($CCl_3F$) working fluid.[1] The heat pipe would self-deploy when heat was applied and the pressure in the heat pipe increased and would retract upon removal of the heat source. Mylar was chosen for the container material due to its high strength and cyclic duty capacity. A 2.54-cm- diam Mylar tube with a 50-$\mu$m wall thickness was fabricated for the container. A flexible epoxy was used to attach the fabric wick to the container in both the evaporator and condenser. An ultralight thermal radiator for lunar and Martian outposts has been designed and fabricated.[2] The heat-pipe container was constructed of a four-ply laminate of Mylar, metal foil, Mylar, and polypropylene that was heat sealed to form a thin walled vacuum tight tube. The metal foil provided the vacuum barrier, and the polymer provided the structural support. The heat pipe was wickless and was designed to operate in the gravity-assist mode on the lunar or Martian surface. Testing confirmed that the radiator rejected a design heat load of 33 W per cell to a heat sink of 50°C.

In most cases, the heat pipes for spacecraft radiators have been rigid. However, in a few cases, heat pipes have been proposed with flexible joints between two rigid portions of the heat pipe. One of the first flexible heat pipes was fabricated with a flexible metal bellows connecting a rigid condenser and evaporator.[3] The heat-pipe performance was degraded approximately 25% in the bent vs straight mode. A second flexible heat pipe was built to carry heat to the moving segment of a thermal switch.[4] The flexible section was made of stainless-steel tubing. A heat pipe with a flexible stainless-steel bellows was fabricated for space radiators by Hwangbo and Joost.[5] The purpose of the flexible segment here was to enable the heat pipe to unfold when deployed in space. Fleischman et al.[6] also designed a heat pipe with flexible joints to enable the heat pipes to be deployed once in space. A deployable space radiator was developed by Aerospatiale and the Centre National d'Etudes Spatiales using heat pipes.[7,8] The radiative panels were fabricated out of aluminum honeycomb and facesheets with five grooved heat pipes embedded in the honeycomb sandwich structure. With a heat load of 245 W, the average temperature drop between the facesheets and heat-pipe vapor was 0.61°C. The temperature of the dissipative units was between −10 and 30°C. The lifetime was designed for a minimum of 10 years, including 3 years storage.

A composite material heat-pipe radiator, where a thin walled titanium tube was wrapped with braided carbon fibers, infiltrated with an epoxy resin (resin transfer molding), and cured has been evaluated.[9] The epoxy bonded the liner to the composite preventing the liner from collapsing under external pressure. The composite material carried the heat-pipe pressure loads, and the titanium liner provided the leak tight container. The heat pipe was 1.4 m long

with a 24-mm diameter with a mass of 0.165 kg, including an initial charge of 20 g of water for the working fluid. The heat pipe used a sintered titanium powder wick in the evaporator with a thickness of 2 mm, a pore radius of 20 $\mu$m, and a permeability of $7 \times 10^{-8}$ m$^2$. No wick was used in the condenser. The heat load dissipated ranged from 10 to 60 W at temperatures ranging from 278 to 403 K. In a separate project, a 4.57-m-long composite-lined titanium tubing was fabricated for use as a heat pipe.[10] An aluminum foil covered with graphite/epoxy (Gr/Ep) design was used to fabricate a loop heat-pipe radiator as an alternative to axially grooved heat pipes.[11] The heat pipe used ammonia as the working fluid and had a porous polyethylene wick in the evaporator with a pore radius of 60 $\mu$m and a permeability of $6.3 \times 10^{-12}$m$^2$. Circumferential and axial grooves were also machined in the wick. The heat pipe, 3.96 m long, was capable of transferring 500 W when at a 2.3-m adverse inclination and 1500 W when horizontal.

Lightweight deployable composite radiators have also been evalauted.[12] These results indicate that high conductivity polymer matrix composites (K1100/Ep) yields dramatic weight savings over aluminum and accommodates high-power-density components. The development of an optimum deployable radiator involves resolving issues related with materials and processing of thermal structural polymer matrix composites (PMCs), bonding heat pipes to PMCs, high-conductance thermal straps, and reliable deployment mechanisms.

An integrated radiator system (IRS) using heat pipes was used to maintain electronics packages within a specified temperature range on the Spacelab Astro-1 payload.[13] The IRS rejected between 308 and 372 W and maintained the radiator surface, which consisted of two orthogonal planes, between $-10$ and 35°C. In addition, the radiator was designed to maintain surface temperatures within 5°C of each other. The heat pipes, spaced 15.2 cm apart, were fabricated out of aluminum and used ammonia (99.997% pure) as the working fluid. Heat pipes were placed on both sides of the radiator panel, and the heat pipes on the back surface were perpendicular to those on the outside surface. This arrangement allowed all of the heat pipes to be thermally connected. The radiating surface was covered with silver-coated clear Teflon® tape giving a solar absorptivity of 0.09 (silver reflecting at solar wavelengths) and an infrared (IR) emissivity of 0.75 (Teflon radiating at IR wavelengths). The heat pipes had maximum leak rates of $3 \times 10^{-8}$ standard cubic centimeters per second (sccs), ensuring a lifetime of several hundred years based on leakage alone.

Two 1.8-m-long heat pipes for the space station were fabricated and tested. One heat pipe used ammonia and one used acetone as the working fluid.[14] In addition, a 6.1-m-long ammonia heat pipe was fabricated and tested. The length of the radiator panels on the space station will be from 7.6 to 15.2 m. The long length limits the use of conventional heat pipe's transport ability. The manufacturers used both a monogroove and a dual-slot heat-pipe construction. A 4.6-m, proof-of-concept, dual-slot heat pipe was fabricated out of stainless steel and used ammonia as the working fluid. The heat pipe attained a heat capacity of 600 W with a tilt of 1 cm. The design transport capacity of the 1.83-m-long heat pipes was 3 kW with ammonia. The heat-pipe operation was found to be very sensitive to test conditions and startup procedures, resulting in dry out, depriming, or unsteady behavior. Several 14.6 m long by 30 cm wide monogroove heat-pipe radiators were also fabricated and tested.[15] The heat pipes were made of 6061-T6 aluminum and charged with ammonia. At an adverse tilt of 0.64 cm, the maximum heat load was between 3000 and 3600 W at 38°C.

The heat pipe evaluated here is made entirely of flexible polymeric materials. The recent growth in the number of moderate temperature polymeric materials makes the flexible heat pipe feasible. When operational, the heat pipe will pressurize and conform to the shape of the channel formed by the webs and facesheets of the radiator panel. The heat-pipe container can be thought of as an impermeable liner, similar to an inner tube on a bicycle tire. The heat pipe fills the entire region between the top and bottom facesheets, thus significantly increasing the through-the-thickness conductivity when compared to a circular heat pipe embedded in a high conductivity material.

The CTE mismatch between the heat pipe and the radiator is a major problem in state-of-the-art radiators. This problem arises due to the use of different materials for the heat pipe and the radiator and the need for intimate thermal contact. Without a flexible, low-modulus material, this can be an insurmountable requirement, i.e., intimate thermal contact between two different high-modulus materials. The use of a flexible heat pipe eliminates the CTE problems and at the same time provides good thermal contact. The flexible heat pipe does not need to be attached to the radiator like a nonflexible heat pipe does. Using conventional heat pipes, the heat pipe must be attached to the radiator to minimize the contact resistance between the heat pipe and the radiator. With a flexible heat pipe, the heat pipe can be inserted into the space made for the heat pipe. When the heat pipe is operational, it will pressurize and obtain good contact with the radiator surfaces. The heat pipes can be used with carbon/carbon, Gr/Ep, or metallic radiators. Unlike many other heat pipes, the CTE of the radiator material is not a major concern when using the flexible heat pipes, and thus the radiator material can be optimized without using the CTE as a constraint.

The heat-pipe application addressed here is for radiators dissipating heat from electronic components that will require the heat pipes to operate in the range of 50°C. This report details the effort to design, fabricate, and test a flexible polymeric heat pipe for space radiators. Two different ultra-high-molecular-weight (UHMW) polyethylene wicks were used and the porosity and permeability were experimentally determined. Mylar, Kapton®, and Teflon were used to fabricate the heat-pipe containers. The test heat pipe was designed and successfully tested.

## Discussion of Results

Several tasks were performed during the course of this work and are discussed in this section. The first task was the selection of the materials to be used for the working fluid, wick, and heat-pipe container. Subsequent tasks included the characterization of the heat-pipe wick, sealing the heat pipe, attaching the wick to the container, heat-pipe design, and heat-pipe testing.

### Material Selection and Compatibility

The materials selection and compatibility consisted primarily of a literature and vendor survey of potential working fluid, container, and wick materials. Long-term (on the order of 10 years) material compatibility between all three components is essential.

*Working Fluid*

The heat-pipe application chosen for this study operates in the 50°C temperature range. Potential working fluids considered are shown in Table 1 along with their operating range and vapor pressure at 50°C. Ammonia is the working fluid that is used in many space radiator applications, but due to its high vapor pressure at 50°C and toxicity, it was not evaluated in this preliminary study. The vapor pressure of water is very low at 50°C, and thus acetone, freon-11, methanol, and ethanol were the only working fluids used. Though ammonia and water are not used, they were considered in regards to compatibility with the wick and container.

*Container*

An extensive vendor and literature survey was undertaken to find container materials that were 1) compatible with one or more of the working fluids for long term exposure at 50°C, 2) impermeable to the vapor phase of the working fluid, 3) flexible, and 4) able to carry the pressure loads. The last requirement, able to carry the pressure loads, is not a firm requirement because in the actual application, the heat pipe would be embedded in a radiator panel that would carry the

**Table 1 Approximate useful range and vapor pressure of several heat-pipe working fluids**

| Working fluid | Range, °C | Vapor pressure at 50°C, kPa (psi) |
|---|---|---|
| Acetone | 0–120 | 79.3 (11.5) |
| Ammonia | −60–100 | 2027 (294) |
| Ethanol | 0–130 | 40.9 (5.93) |
| Freon 11 | −40–120 | 236.5 (34.3) |
| Methanol | 10–130 | 52.3 (7.58) |
| Water | 30–200 | 12.2 (1.77) |

loads. A final requirement was that the container material be readily available and could be made into a heat-pipe container with minimal development, i.e., in a short amount of time and at a low cost.

An extensive set of design handbooks for plastics[16] was used to assist in the compatibility evaluations. The Plastics Design Library rating is a weighted value of a materials resistance after exposure to a specific environment. The factors that are considered are changes in the weight, diameter or length, thickness, volume, mechanical properties, and visual appearance. Values from 1 to 9 are given to each material, with a 9 meaning the materials are extremely compatible.

Though Teflon, Kapton, and Mylar meet several of the listed requirements, none meets all of the requirements. None of the polymeric films has the desired impermeability. Strength is also a problem for Teflon, having a tensile strength of 20.6 MPa (3,000 psi), compared to Mylar and Kapton at 200 MPa (29,000 psi) and 231 MPa (33,500 psi), respectively. It was determined that a laminate would provide the optimal properties. Teflon, the most inert of the polymers, should be on the inside for compatibility, a thin film of a metallic foil should next be used to reduce vapor permeability, and Mylar or Kapton should be used as an outer layer for strength.

The tubes were made by spiral wrapping the several plies around a mandrel. The inner ply, thus, had a seam that may be a problem from the material compatibility point of view. The plies were staggered by approximately 25% of a ply width. The first tube, and the most standard product line, was a four-ply tube, with the plies being Teflon coated Kapton. DuPont, the manufacturer of Kapton, Mylar, and Teflon, laminates Teflon on Kapton but not on Mylar. The purpose of laminating Teflon on Kapton is so that the Kapton can be heat sealed. The heat sealing temperature of the Teflon is above the reuse temperature of Mylar, and, thus, Mylar is not laminated with Teflon. The inside lamina was Kapton laminated on both sides with Teflon, referred to as TKT. Three plies of TKT were used. Thus the tube was constructed as

$$\text{TKT} + \text{TKT} + \text{TKT}$$

Each ply was 51 $\mu$m thick, with the Kapton being 25 $\mu$m thick and the Teflon layers being 13 $\mu$m thick. The total thickness of the tube was, thus, 152 $\mu$m. The Teflon layers were heat sealed together, resulting in a tube with Teflon on the inside and Kapton on the outside. The final material cross section is given by TKTKTKT. The tube was thicker than is likely to be required for a space radiator, but for the benchtop tests, a thicker tube was used for safety purposes. In the benchtop tests, the heat-pipe container was not supported by another structure as it would be in the space radiator, where the radiator facesheets and webs support the heat pipe.

The second tube consisted of Mylar and aluminized Mylar (AM) in addition to an inner ply of Teflon-laminated Kapton. Because the Mylar (polyester) cannot be heat sealed, it was bonded with an isocynate polyester adhesive. The tube was constructed as

$$\text{TK} + \text{AM} + \text{AM} + \text{M} + \text{KT}$$

The TK was 38 $\mu$m thick and the Mylar and AM layers were 25 $\mu$m thick. The adhesive was used between each layer, and no heat sealing was performed. The total thickness of the components prior to fabrication was 178 $\mu$m.

*Wick*

Two different materials were utilized for the wick. One wick material was a porous UHMW polyethylene film with available thicknesses ranging from 0.013 to 0.318 cm. The film wicks, which are produced by sintering powders, have a porosity of approximately 30%. The porous films were plasma treated to render them hydrophilic, producing an excellent wicking material. The films can also be treated with a surfactant, which is less costly than the plasma treatment.

Several formed UHMW polyethylene wicks were also obtained for evaluation. The wicks were 0.7–0.8 m long with a 2.54-cm outer diameter and 1.6-cm inner diameter. The porosity was estimated by the manufacturer to be 25% with an average pore size (diameter, though the pores are not circular) of 20 $\mu$m. The 0.8-m-long formed wick, with an outer diameter of 2.54 cm and an inner diameter of 1.6 cm, had a mass of 150 g. The resin used to make the wick had a specific gravity of 0.93. If the wick was full density, the total mass would be 233 g. With a mass of 150 g, the void space is 36%.

**Preventing Collapse of the Wick**

The heat-pipe wick needs to remain located next to the outer container during operation. A thin gap between the wick and the container is acceptable. However, a large gap is not. As a result, care must be taken to ensure that the wick and the container remain close to each other during operation. If the wick and container are not attached, it is possible that the external pressure on the heat pipe may collapse the heat-pipe container prior to operation (when there is vacuum inside). If this occurs, it is essential that the wick follows the container back to the original shape when pressurized. Because the wick is porous, it will not necessarily take its original shape merely by pressurization of the heat pipe.

Several alternatives exist for maintaining the wick in close proximity to the container. The first is to have a wick that is structurally capable of maintaining its shape with a vacuum on the inside. The formed wicks, with a 0.48-cm-thick wall, have the required rigidity to withstand atmospheric pressure on the outside and vacuum on the inside without collapsing. However, for a lightweight space radiator application, the formed wick used here may be too heavy.

A second technique to maintain the wick in close proximity to the container is to attach the wick to the container. A 2.54-cm-wide roll of porous UHMW film was used as the first layer wrapped around a mandrel, thus forming the inside layer of the tube. The Mylar and Kapton strips were wrapped and bonded over the porous UHMW film. The wick was bonded to the tube because the UHMW cannot withstand the high temperatures required for heat sealing. The final product was a Mylar/Kapton tube with the porous UHMW wick bonded to the inside.

The third technique is to insert a support structure, such as a spring, in the heat pipe. The primary disadvantage of this technique is the weight penalty and potential compatibility problems.

**Property Characterization**

Several properties of the wick and container were determined to assist in characterization of the heat pipe. The permeability and capillary radius of several wicks were determined, as was the burst pressure of the containers. Water was not included as one of the working fluids tested because the currently used wicks did not wick water.

*Permeability and Capillary Radius*

The wick effective capillary radius and permeability were determined by measuring the rate of rise of liquid in the wick. The equation governing the rate of rise of the liquid is given by

$$\frac{\mathrm{d}x}{\mathrm{d}t} = \frac{K}{\varepsilon \mu_l} \frac{2\sigma \cos\theta}{r_p} \frac{1}{x} - \frac{K}{\varepsilon \mu_l} \rho_l g \sin\beta \tag{1}$$

A plot of $\mathrm{d}x/\mathrm{d}t$ vs $1/x$ should be a straight line with the permeability determined from the intercept and $r_p$ determined from the slope.

The apparatus shown in Fig. 1 was used to determine the permeability and effective capillary radius. On the left-hand side of Fig. 1 is the wick inside of a glass cylinder. A transparent ruler was attached to the cylinder to help record the wicking height. An additional ruler was used to eliminate parallax. The short cylinder on the right contained the working fluid. Between the two cylinders are the valves and lines to pull a vacuum on the long cylinder and to put the liquid into the large cylinder.

The formed UHMW wick was tested with acetone as the working fluid. Acetone was put into the cylinder with the wick, and the clock was started. The acetone wicked up about 5 cm almost immediately. The first datum point obtained was at 6.4 cm at 15 s. The time was recorded at 1.3-cm wicking height increments. The data were then plotted as already mentioned and curve fit linearly. The linear curve fit for the data is

$$\frac{\mathrm{d}x}{\mathrm{d}t} = a_0 + a_1 \left( \frac{1}{x} \right) \tag{2}$$

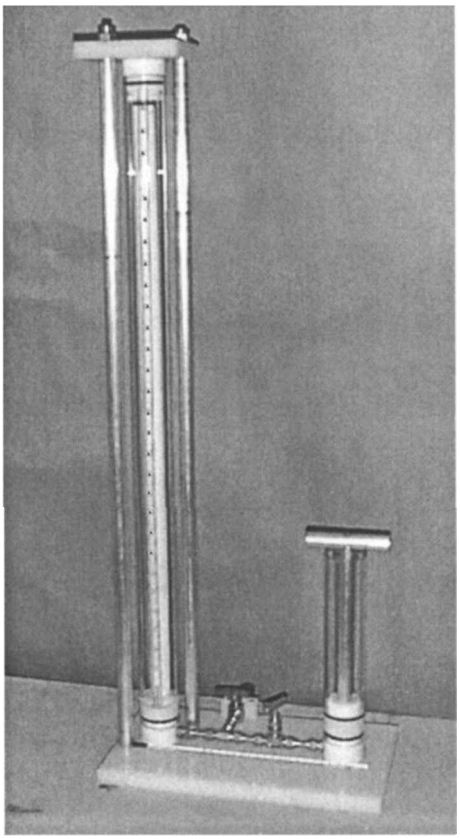

**Fig. 1 Photograph of apparatus used for determination of permeability and pore radius.**

where $a_0 = -3.243 \times 10^{-3}$ cm/s and $a_1 = 1.436 \times 10^{-2}$ cm$^2$/s. The permeability and capillary radius were obtained from

$$-(K/\varepsilon\mu_l)\rho_l g \sin\beta = -3.243 \times 10^{-3}\text{cm/s} \tag{3}$$

$$\frac{K}{\varepsilon\mu_l}\frac{2\sigma\cos\theta}{r_p} = 1.436 \times 10^{-2}\,\text{cm}^2/\text{s} \tag{4}$$

Because the wick was vertical, $\sin\beta = 1$. The porosity was estimated by the manufacturer to be ~25%. Weight and density calculations estimated the porosity to be 36%. However, to be conservative, the 25% value was used. The liquid kinematic viscosity of acetone at the test temperature of 18°C is $0.4612 \times 10^{-6}$ m$^2$/s, and the density is $0.7874 \times 10^3$ kg/m$^3$. The permeability was, thus, $2.24 \times 10^{-8}$ cm$^2$.

The determination of the capillary radius requires the contact angle. The contact angle is extremely difficult to measure accurately, and with a value $0 < \theta < 15$ deg, $\cos\theta$ is between $1 > \cos\theta > 0.966$. In a 1957 study by Zisman,[17] the cosine of the contact angle is given as a function of the surface tension. For each of the working fluids studied here, the surface tension is in the range of 0.02–0.025 N/m, giving a value of $\cos\theta$ very near 1.0. A value of $\cos\theta = 0.98$ is used here, giving an error of <2%. The surface tension is 0.02301 N/m, and the dynamic viscosity is $3.2984 \times 10^{-4}$ kg/m-s. The capillary radius is then 20.45 $\mu$m, compared with the average pore size of 20 $\mu$m estimated by the manufacturer. The pumping is determined by the largest pore size. It is, thus, expected that capillary radius will be larger than the average pore size. Three more wicking tests were performed on the same wick, again with acetone.

The permeability and capillary radius were also calculated for the formed UHMW wick with ethanol and methanol. There appeared to be less scatter in the methanol and ethanol data than in the acetone data. Freon 11 was also tested with the formed UHMW wick. The freon caused major swelling of the wick, validating the incompatibility of these two materials. As a result, only one test was performed with this wick and freon. The capillary radius and permeability values are summarized in Table 2 for each working fluid.

A UWMW film wick (D/W 472P) was also evaluated. It was a flat sheet of porous material with a thickness of 0.075 cm. Two different surface treatments, referred to as A and B, were tested.

**Table 2 Average experimentally determined permeability and capillary radius values**

| Fluid | Film wick | Formed wick |
|---|---|---|
| Acetone | | |
| Permeability, cm$^2$ | $5.61 \times 10^{-8}$ | $3.70 \times 10^{-8}$ |
| Capillary radius, $\mu$m | 22.58 | 20.91 |
| Ethanol | | |
| Permeability, cm$^2$ | $1.56 \times 10^{-7}$ | $7.52 \times 10^{-8}$ |
| Capillary radius, $\mu$m | 32.90 | 27.1 |
| Freon 11 | | |
| Permeability, cm$^2$ | $8.37 \times 10^{-8}$ | $3.01 \times 10^{-8}$ |
| Capillary radius, $\mu$m | 23.65 | 17.65 |
| Methanol | | |
| Permeability, cm$^2$ | $1.13 \times 10^{-7}$ | $5.16 \times 10^{-8}$ |
| Capillary radius, $\mu$m | 28.14 | 24.12 |

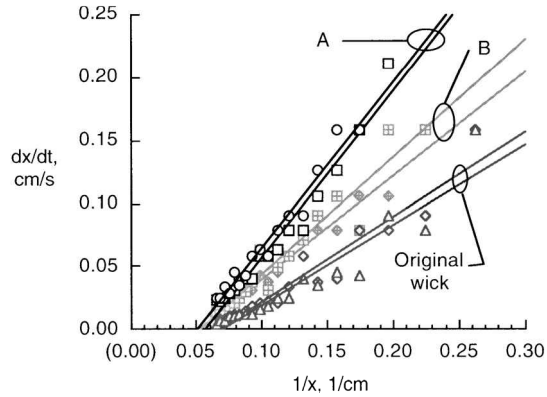


**Fig. 2 Plot of wicking height data used for permeability and capillary radius calculation for film wick with surface treatments A and B and with acetone as the working fluid.**

Both treatments were a plasma treatment that is proprietary to the manufacturer. A plot of the wicking height data is shown in Fig. 2 for both surface treatments. The wick with the standard surface treatment was also tested and is also shown in Fig. 2. From an analysis of the data, it is evident that surface treatment A wicked better than surface treatment B or the original wick. The film wick was also evaluated with freon 11, ethanol, and methanol. As with the formed wick, significant swelling was noticed with freon 11. The capillary radius and permeability values are summarized in Table 2 for each working fluid.

*Capillary Radius*

The capillary radius in the wicks was also determined by a bubble test, where the wick was pressurized and the pressure causing bubbles to emerge from the wick was related to the capillary radius. The apparatus used to measure the permeability was inverted on its side, and a few minor modifications were made to perform the bubble test. The pressure corresponding to the first bubble to emerge from of the wick can be related to the largest capillary radius, and the pressure corresponding to a constant stream of bubbles all over the wick can be related to an average capillary radius. A photograph of the apparatus used for the bubble test is shown in Fig. 3. A mercury manometer, not shown in the photograph, was used to determine the pressure.

The bubble tests were performed with methanol in the cylinder and argon as the pressurization gas. The argon was supplied from a high-pressure gas bottle, and the pressure differential was measured with a mercury manometer. The formed UHMW wick was tested, but the film wick was not tested because it was a flat sheet. At a pressure of 16-mm Hg, no bubbles were present. At 17–18-mm Hg, bubbles started, and at 32-mm Hg, bubbles were emerging over the entire wick. The capillary radius can be determined from

$$r_p = \frac{2\sigma\cos\theta}{P} \tag{5}$$

Again taking $\cos\theta = 0.98$ and using a surface tension of 0.2246 N/m at 295 K, the capillary radius corresponding to 17-mm Hg was

**Table 3 Results of heat-pipe container burst tests**

| Tube | Environment | Burst pressure, kPa (psi) |
|---|---|---|
| AM | Atmospheric air | 1241 (180) |
| AM | 50°C water | 965 (140) |
| AM | 50°C water | 931 (135) |
| Kapton | Atmospheric air | 689 (100) |
| Kapton | 50°C water | 724 (105) |

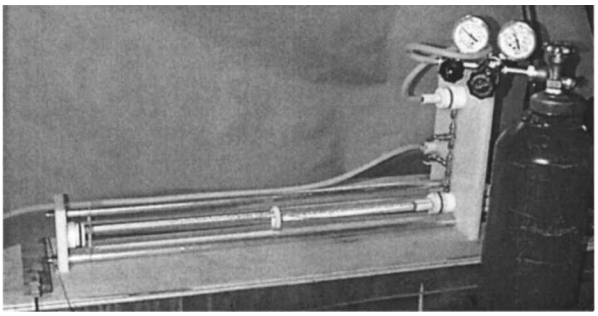

**Fig. 3 Photograph of the apparatus used for the bubble test to determine wick capillary radius.**

19.4 $\mu$m. This represents the largest capillary radius and corresponds quite well to the capillary radius obtained from the permeability tests. The capillary radius corresponding to 32-mm Hg was 10.3 $\mu$m.

*Burst Pressure*

The AM tube and the Kapton tube were burst tested to determine the strength of the spirally wound and bonded tubing, with the results listed in Table 3. In each case, aluminum plugs were bonded in the ends of the tube and held in place with hose clamps. The length of the tube between the plugs was 12.7 cm. The tubes were tested both in atmospheric air and in 50°C water. The 50°C water tests were performed to see if the strength was significantly changed at an elevated temperature.

From the results of the tests, it appeared that the AM tube was stronger than the Kapton tube even though Kapton is known to have a slightly greater strength than Mylar. The Kapton tube was fabricated by heat sealing Teflon. Thus, Teflon was the adhesive in the Kapton tube. Teflon has a much lower strength than either Kapton or Mylar. The AM tube was bonded together with a polyester adhesive (Mylar is a polyester). The section of tube split open at the seams, indicating that the material strength was stronger than the bond.

**Heat-Pipe Design**

The heat-pipe concepts evaluated in this effort can be utilized in nearly any moderate temperature heat pipe. However, for evaluation purposes, a current space radiator application was chosen for which the heat-pipe effort is directed. The experimental effort attempted to validate the concept of using a flexible polymeric heat pipe and not to demonstrate a design for the radiator application. The heat pipe tested used a 0.76-m-long formed UHMW polyethylene wick. The wick was stated by the manufacturer to have an average pore size of 20 $\mu$m and a porosity of 25%. Experimental tests established a capillary radius, but were not attempted for the porosity. The outer diameter of the wick was 2.54 cm, and the inner diameter was 1.59 cm, giving a wall thickness of 0.48 cm.

The heat-pipe design code HTPIPE was used for the design work.[18] The wick geometry and properties are input into HTPIPE along with the evaporator and condenser lengths. The working-fluid properties are calculated in the program. An example of the program output is given in Tables 4 and 5 for evaporator exit temperatures $T_e$ ranging from 300 to 350 K. The capillary pressure is the total pressure generated in the wick and is equal to the sum of all of the other pressure drops. All of the pressure values are given in units of dynes per square centimeter. The capillary pressure is equal to $2\sigma/r_p$. The liquid-pressure drop is the pressure drop in the wick, and the hydrostatic-pressure drop is the liquid-pressure drop due to inclination of the heat pipe. In Table 4 liquid-pressure drops are given first. The hydrostatic-pressure drops are all zero and are not shown. Vapor-pressure drops are given in the evaporator and condenser regions. Vapor-pressure drops in the adiabatic regions (which are not shown) are all zero. In Table 5, temperatures are the temperatures at the beginning of the evaporator ($T_{be}$) and condenser ($T_{bc}$) and at the beginning of the evaporator ($T_{beson}$) and condenser ($T_{bcson}$) at the sonic limit and are given in units of Kelvin.

**Table 4 HTPIPE output: pressure drops**

| | Liquid, dynes/cm$^2$ | | Vapor, dynes/cm$^2$ | |
|---|---|---|---|---|
| $T_e$ | Capillary | Liquid | Evaporator | Condenser |
| 300 | 21,071 | 21,060 | 3 | 7 |
| 310 | 19,982 | 19,975 | 2 | 5 |
| 320 | 18,860 | 18,856 | 1 | 4 |
| 330 | 17,711 | 17,707 | 1 | 3 |
| 340 | 16,537 | 16,534 | 1 | 2 |
| 350 | 15,345 | 15,342 | 1 | 2 |

**Table 5 HTPIPE output: temperature and power limits**

| Temperature, K | | | | Power limits, W | | |
|---|---|---|---|---|---|---|
| $T_{be}$ | $T_{beson}$ | $T_{bc}$ | $T_{bcson}$ | $q_{sonic}$ | $q_{ent}$ | $q_{cap}$ |
| 300 | 318 | 300 | 300 | 2,375 | 1,683 | 5 |
| 310 | 329 | 310 | 310 | 3,424 | 1,917 | 5 |
| 320 | 341 | 320 | 320 | 4,836 | 2,155 | 5 |
| 330 | 352 | 330 | 330 | 6,702 | 2,396 | 4 |
| 340 | 364 | 340 | 340 | 9,116 | 2,637 | 4 |
| 350 | 376 | 350 | 350 | 12,171 | 2,872 | 4 |

The four heat flux power limits are also given in Table 5. The sonic, entrainment, and capillary limits are all axial limits, whereas the boiling limit (not shown) is a radial limit. With an input heat flux of 220 W, the sonic, entrainment, capillary, and boiling limits are all satisfied if they are greater than 220 W.

For the case given in Tables 4 and 5, the hydrostatic pressure drops are zero because the tilt angle is 0 deg. The adiabatic vapor pressure drop is zero because the adiabatic length is 0 cm. The sonic and entrainment limits are met at each temperature because the values are greater that 220 W. The capillary limit (Table 5) is not met and cannot be met for this particular condition, i.e., wick, working fluid, and heat flux. Thus, further design would be necessary to fabricate a heat pipe that would operate properly at these conditions. The boiling limit is not met here and cannot be met with this wick and a heat flux of 220 W. However, the heat pipe can be run even if the boiling limit is not met, though one would not want to design an actual space radiator heat pipe that way. To meet and calculate the boiling limit, a thinner wick is required as well as an accurate value for the nucleation site radius.

The heat-pipe limits were checked for four different working fluids: methanol, ammonia, acetone, and freon-11. For each of the four working fluids, the sonic and entrainment limits were easily satisfied. As with the example in Tables 4 and 5, the sonic and entrainment limits were well above 220 W. The capillary limit, however, was not satisfied at 220 W for any of the working fluids. However, as shown in Fig. 4, methanol permits the highest heat flux while still satisfying the capillary limit. At an operating temperature of 400 K, a throughput of 60 W (defined as the axial heat flux transferred by the heat pipe) can be tolerated without exceeding the capillary limit. The suggested maximum use temperature for the UHMW wick was 80°C or 353 K. Therefore, a throughput of 45–50 W was the maximum throughput that can be tolerated and satisfy the capillary limit. As a result of this design, the heat pipes used methanol as the working fluid with a throughput of 45–50 W.

An attempt was made to fabricate a wick that would satisfy both the capillary and boiling limits. A schematic drawing of the wick is shown in Fig. 5. The shaded area is the porous wick material. The three circles represent the liquid arteries, and the large open space represents the vapor space. The wick has three arteries to help increase the pumping capability and increase the capillary limit, thus

enabling the heat pipe to operate without violating the capillary limit. The way to satisfy the boiling limit is to have a very thin wick and, thus, reduce the thermal resistance through the wall and wick into the heat pipe. The wick design shown in Fig. 5 attempts to minimize the wick thickness where heat is input. The quadrant where there is no artery was fabricated as thin as reasonably possible without initiating a development effort. Though the wick shown in Fig. 5 may not enable the heat pipe to operate within the capillary and boiling limits, it did incorporate the required design features to the maximum extent possible without more detailed manufacturing studies.

The 45–50-W throughput must be removed from the condenser. Natural convection from a vertical cylinder with a length of 0.64 m and a diameter of 2.54 cm would remove ~200 W. This value is obtained from an empirical relation for the heat transfer coefficient from a vertical cylinder. The Grashof number was approximately $1.3 \times 10^9$, indicating the flow was just turbulent. The heat transfer coefficient was then obtained from

$$hL/k = 0.1(Gr \cdot Pr)^{\frac{1}{3}} \tag{6}$$

The heat transfer coefficient was calculated to be 4.1 W/m$^2$K. With a $\Delta T$ of 25 K between the wall and the ambient temperatures, a heat flux of ~200 W could be removed by natural convection. Thus, natural convection was able to remove all of the heat from the heat pipe without supplemental cooling. In addition, a small amount of heat was radiated from the heat-pipe surface, further contributing to the heat loss.

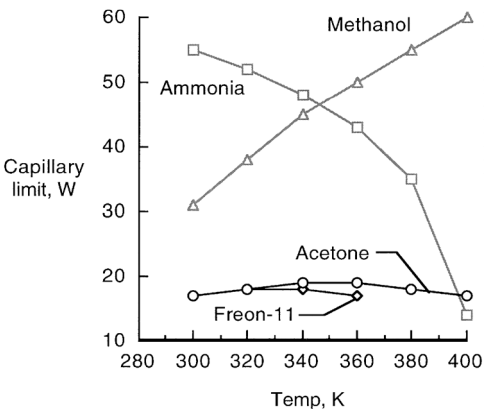


**Fig. 4 Capillary limit as a function of temperature and working fluid.**

**Heat-Pipe Test**

Eight heat pipes were fabricated as already discussed. The sealing technique was able to adequately seal several of the heat pipes, but was not consistent enough or lightweight enough to be used on actual radiator heat pipes. The heat pipes were made with different combinations of the containers and wicks as listed in Table 6. Several of the heat pipes did not hold a vacuum when they were evacuated prior to charging with methanol. The 0.2-cm-thick wick with three arteries collapsed several hours after a vacuum had been pulled on the heat pipe. The wick failed in the quadrant with no artery, where the wick was only 0.2 cm thick. Thus, any further tests with that wick should be performed with the heat pipe in a vacuum until the heat pipe is heated and the internal vapor pressure rises enough to prevent failure of the wick. For a space application, with vacuum on the outside, collapse of the wick would not be a problem. The 0.075-cm-thick film wick that was bonded to the container flattened upon pulling a vacuum in the heat pipe. However, on repressurization, the heat pipe returned to its cylindrical shape.

After the heat pipes were fabricated, methanol was introduced into the heat pipes. The wick, with a 2.54-cm outer diameter, a 0.79-cm inner diameter, and a 0.76-m length, had a volume of 0.88 cm$^3$. The wick porosity was estimated by the manufacturer to be 25%. However, a weight estimate resulted in a porosity of 36%. To be on the conservative side, 36% was used. That resulted in 5.17 in.$^3$ (84.7 cm$^3$) of methanol. With a room temperature density of 0.784 g/cm$^3$, and a 10% excess, approximately 73 g of methanol, was required. At the operating temperature of 323 K, the density of methanol was reduced about 2%, thus requiring the use of a portion of the excess methanol. After the heat pipes were charged with the methanol, they were returned to Analytical Services and Materials, Inc., where they were tested.

**Table 6 Description of the heat pipes fabricated**

| Container | Wick | Result |
|---|---|---|
| Kapton | 0.48-cm wall, no artery | Held moderate vacuum |
| Kapton | 0.48-cm wall, no artery | Held vacuum very well |
| AM | 0.48-cm wall, no artery | Did not hold vacuum |
| AM | 0.48-cm wall, no artery | Did not hold vacuum |
| Kapton | 0.2-cm wall, artery | Wick collapsed under pressure |
| Kapton | 0.075-cm wall, bonded to wall | Wick collapsed, did not hold vacuum |
| AM | 0.2-cm wall, artery | Did not hold vacuum |
| AM | 0.075-cm wall, bonded to wall | Wick flattened, did not hold vacuum |

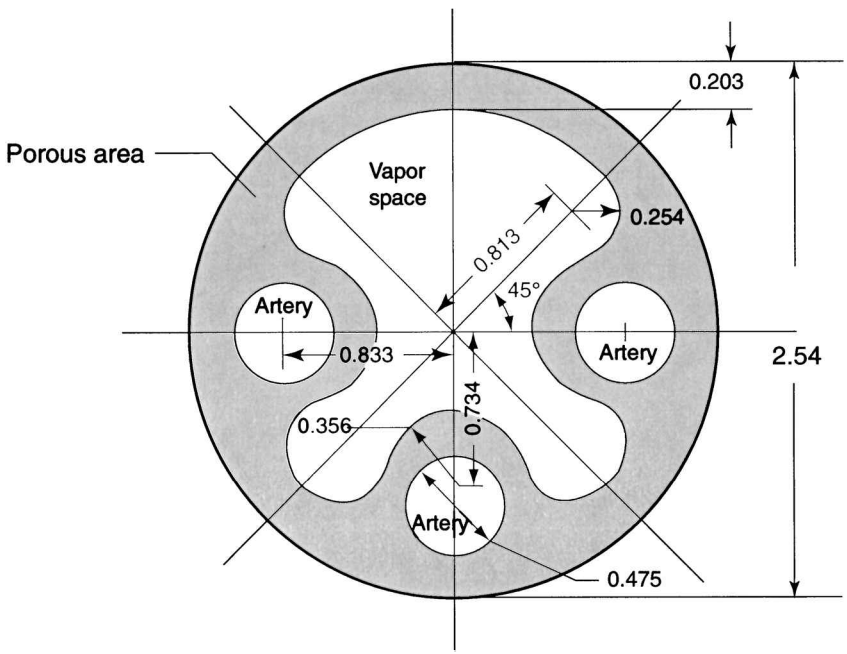


**Fig. 5 Schematic of wick with three arteries not at the heated surface. (All lengths are in centimeters.)**

Two heat pipes, 1 and 2, were tested. The heat pipes were oriented both vertically and horizontally and heated over the first 8 in. (20 cm) of the heat pipe. The heat pipes were heated with resistance heaters that were wrapped around approximately 20 cm of the heat pipe. Fibrous insulation was placed over the heaters. Approximately 35 W was output from the heaters based on a voltage (40 V) and heater resistance (46.1Ω). Thermocouples were bonded and strapped with tie wraps to the outer surface of the containers. The thermocouples were located 10 cm apart for most of the condenser length, but were located 2.5 cm apart near the end of the heat pipe to evaluate any effect of noncondensable gas (NCG). NCG can be the result of either air in the heat pipe or the result of gas generation in the heat pipe due to noncompatible materials.

Heat pipe 1 held a vacuum moderately well but did have a leak and, thus, had air in the heat pipe. As a result, the heat pipe operated only over a portion of its length, as shown by the steady-state temperatures in Fig. 6. Two different steady-state temperature distributions are shown, which are representative of the data taken at two times. In most all cases, the second thermocouple (at $x = 33$ cm) indicated a temperature 5–10°C lower than the neighboring thermocouples. A short isothermal region was noticed, with a sharp temperature drop to nearly ambient temperature in the NCG region. The temperature distributions shown here are consistent with what one would expect from a heat pipe that contained NCG. In this heat pipe, the NCG was air that entered the heat pipe because it could not hold a vacuum.

Heat pipe 2 held a vacuum quite well and operated nearly isothermally over the entire length of the heat pipe. Figure 7 shows representative temperature distributions corrected for ambient temperature thermocouple differences. There was a 6°C difference between the maximum and minimum ambient temperature readings. At each thermocouple location, the difference between the ambient temperature and the minimum ambient temperature was subtracted from the operating temperature. For example, the ambient temperature at the first thermocouple, $x = 23$ cm, was 18°C, whereas the minimum ambient thermocouple reading was 12°C. Thus, 6°C was subtracted from the thermocouple reading at $x = 23$ cm during operation (74°C) to obtain a normalized temperature of 68°C. Thus, the temperature distribution shown in Fig. 7 omits a portion of the wide variation in ambient temperatures resulting from different thermocouples. Three different temperature distributions are shown in Fig. 7. The first one, from day 3, is shown by the circles and is relatively isothermal. By day 5, the end of the heat pipe was cooler than the rest of the heat pipe, most likely due to NCG or loss of working fluid. The NCG could be due to gas generation in the pipe (due to chemical incompatibilities) or air leakage into the pipe. On day 6, the pipe was oriented horizontally. At that time, two leaks were noticed in the heat pipe. It is uncertain when the leaks occurred. The horizontal temperature distribution is shown by the triangles and is relatively uniform until it drops to ambient temperatures. It is uncertain whether the drop in temperatures (nonisothermal operation) is due to 1) air in the heat pipe, 2) NCG in the heat pipe, 3) insufficient supply of working fluid, or 4) exceeding the capillary limit.

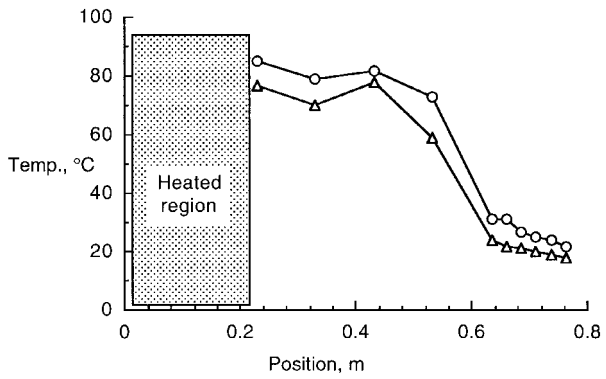


**Fig. 6 Representative steady-state temperature distributions in heat pipe 1.**

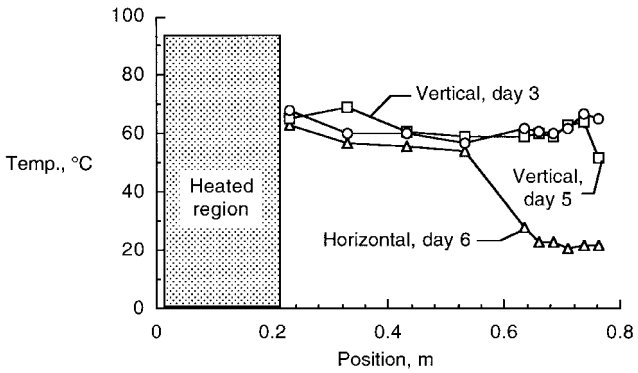


**Fig. 7 Representative steady-state temperature distributions in heat pipe 2.**

## Conclusion

This study has demonstrated the feasibility of fabricating flexible polymeric heat pipes that may be used in spacecraft radiators. Two UHMW polyethylene wicks were characterized regarding permeability and capillary radius. Heat-pipe containers were fabricated out of AM and Kapton laminates. In each case, thin plies were wrapped around a mandrel and bonded together. Burst tests on the containers indicated a burst pressure far exceeding the required vapor pressures of the heat pipes. Three heat pipes were tested with varying degrees of heat-pipe operation achieved.

The successful fabrication and operation of the heat pipes has demonstrated that the flexible polymeric heat pipe is feasible. The next step would be to optimize the heat pipe for use in a space radiator. From preliminary design studies, it appears that the design of a wick such that the capillary and boiling limits are satisfied is the primary challenge.

## Acknowledgments

This work was supported by NASA Langley Research Center under a Phase I Small Business Innovative Research Contract NAS1-97080. The support of Wallace L. Vaughn, NASA Langley Technical Monitor, is greatly appreciated. The assistance of Jay Ochterbeck of Clemson University, for filling the heat pipes, and Stone Industrials, College Park, Maryland, for fabricating the containers, is greatly appreciated. Wicks used for the heat pipes were obtained from De-Wal Industries (film wick), Saunderstown, Rhode Island, and from Pore Technology, Inc. (formed wick), Framingham, Massachusetts.

## References

[1]Woloshun, K. A., "Membrane Heat Pipe Space Radiator Design," 6th International Heat Pipe Conf., Grenoble, France, 1987; also Los Alamos National Lab., Rept. LA-UR-87-969, Los Alamos, NM, 1987.

[2]Garner, S. D., and Gernert, N. J., "Ultralight Thermal Radiator," NASA Tech Briefs, Jan. 1997, p. 72.

[3]Bliss, F. E., Jr., Clark, E. G., Jr., and Stein, B., "Construction and Test of a Flexible Heat Pipe," American Society of Mechanical Engineers, ASME Paper 70HT/SPT-13, June 1970.

[4]Wolf, D. A., "Flexible Heat Pipe Switch," Dynatherm Corp., Final Rept., DTM-81-8, NAS5-25568, Hunt Valley, MD, Oct. 1981.

[5]Hwangbo, H., and Joost, T. E., "A Flexible Variable Conductance Heat Pipe Design for Temperature Control of Spacecraft Equipment," AIAA Paper 88-2680, June 1988.

[6]Fleischman, G., Blasiulis, A., and Gottschlich, J., "Advanced Heat Pipe Components for High Power Spacecraft Thermal Management," AIAA Paper 90-0058, Jan. 1990.

[7]Amidieu, M. M., Moschetti, B., and Tatry, M. B., "Development of a Space Deployable Radiator Using Heat Pipes," Aerospatiale, N88291281XSP, Paris, March 1988.

[8]Moschetti, B., Amidieu, M. M., and Tatry, M. B., "Design and Test of a Space Deployable Space Radiator," Aerospatiale, Rept. SNIAS-861-440-103; ETN-86-97612, Paris, 1986.

[9]Garnert, N. J., Sarraf, D. B., Guenther, R. J., and Hurlbert, K. M., "Composite Material Heat Pipe Radiator," *Space Technology and Applications Forum (STAIF-96) Proceedings of the 1st Conference on Next Generation Launch Systems and 2nd Spacecraft Thermal Control Symposium*, Pt. 2, No. 361, American Inst. of Physics, Woodbury, NY, 1996, pp. 753–763.

[10]Garnert, N. J., Sarraf, D. B., Armstrong, D. L., and Blood, S. A., "Aluminum Foil Lined Composite Tubing," *Space Technology and Applications Forum (STAIF-96) Proceedings of the 1st Conference on Next Generation Launch Systems and 2nd Spacecraft Thermal Control Symposium*, Pt. 2, No. 361, American Inst. of Physics, Woodbury, NY, 1996, pp. 889–894.

[11]Garnert, N. J., and Sarraf, D. B., "Loop Heat Pipe Radiator," *Space Technology and Applications Forum (STAIF-96) Proceedings of the 1st Conference on Next Generation Launch Systems and 2nd Spacecraft Thermal Control Symposium*, Pt. 2, No. 361, American Inst. of Physics, Woodbury, NY, 1996, pp. 721–729.

[12]Kriegbaum, R., and Rawal, S. P., "Thermal-Structural Composites Radiator Trends," *Space Technology and Applications Forum (STAIF-96) Proceedings of the 1st Conference on Next Generation Launch Systems and 2nd Spacecraft Thermal Control Symposium*, Pt. 2, No. 361, American Inst. of Physics, Woodbury, NY, 1996, pp. 875–880.

[13]Hamner, R. M., and Hornsby, L. S., "Flight Performance of the Spacelab Astro-1 Mission Integrated Radiator System," *Society of Automotive Engineers Transactions*, Vol. 100, Sec. 1, Pt. 2, 1991, pp. 1876–1886.

[14]Carlson, A. W., Gustafson, E., and Roukis, S. L., "High Thermal-Transport Capacity Heat Pipes For Space Radiators," 17th Intersociety Conf. on Environmental Systems, Rept. 871509, Seattle, WA, July 1987.

[15]Brown, R., Gustafson, E., Gisondo, F., and Hutchison, M., "Performance Evaluation of the Grumman Prototype Space Erectable Radiator System," AIAA Paper 90-1766, June 1990.

[16]*Plastics Design Library*, Andrew Hill, 1994.

[17]Zisman, W. A., "Relation of Chemical Constitution to the Wetting and Spreading of Liquids on Solids," NRL Rept. 4932, May 1957.

[18]Woloshun, K. A., Merrigan, M. A., and Best, E. D., "HTPIPE: A Steady-State Heat Pipe Analysis Program," Los Alamos National Lab., Rept. LA-11324-M, Los Alamos, NM, Nov. 1988.

I. E. Vas
*Associate Editor*